Current Biology, Vol. 15, 68–72, January 11, 2005, ©2005 Elsevier Ltd. All rights reserved. DOI 10.1016/j.cub.2004.12.065

Yeast Nhp6A/B and Mammalian Hmgb1 Facilitate the Maintenance of Genome Stability

Sabrina Giavara,[1] Effie Kosmidou,[2] M. Prakash Hande,[3] Marco E. Bianchi,[4] Alan Morgan,[2] Fabrizio d'Adda di Fagagna,[1,5] and Stephen P. Jackson[1,*]

[1]The Wellcome Trust and Cancer Research UK Gurdon Institute and Department of Zoology
University of Cambridge
Tennis Court Road
Cambridge CB2 1QN
United Kingdom

[2]The Physiological Laboratory
University of Liverpool
Crown Street
L69 3BX Liverpool
United Kingdom

[3]Department of Physiology and Oncology Research Institute
Faculty of Medicine
National University of Singapore
Block MD9
2 Medical Drive
Singapore 117597
Singapore

[4]San Raffaele University
Via Olgettina 58
20132 Milano
Italy

Summary

Saccharomyces cerevisiae **Nhp6A and Nhp6B are chromatin architectural factors that belong to the high-mobility group box (HMGB) superfamily and appear to be functionally related to mammalian Hmgb1 [1]. They bind to the minor groove of double-stranded DNA in a non-sequence-specific manner [2] and thereby influence chromatin structure [3]. Previous work has implicated these proteins in a variety of nuclear processes, including chromatin remodeling, DNA replication, transcription, and recombination [4–10]. Here, we show that Nhp6A/B loss leads to increased genomic instability, hypersensitivity to DNA-damaging agents, and shortened yeast cell life span that is associated with elevated levels of extrachromosomal rDNA circles. Furthermore, we show that hypersensitivity toward UV light does not appear to reflect a decreased capacity for DNA repair but instead correlates with higher levels of UV-induced thymine dimer adducts being formed in cells lacking Nhp6A/B. Likewise, we show that mouse fibroblasts lacking Hmgb1 display higher rates of damage after UV irradiation than wild-type controls and also exhibit pronounced chromosomal instability. Taken together, these data indicate that Nhp6A/B and Hmgb1 protect DNA from damaging agents and thus guard against the generation of genomic aberrations.**

*Correspondence: s.jackson@gurdon.cam.ac.uk

[5]Present address: IFOM Foundation-The FIRC Institute of Molecular Oncology Foundation, Via Adamello 16, 20139 Milan, Italy.

Results and Discussion

To explore the potential roles of non-histone proteins 6 A/B (Nhp6A/B) in the DNA damage response, we tested the sensitivity of a *nhp6a/b* double mutant strain toward a range of genotoxic agents. As shown in Figures 1 and S1 (in the Supplemental Data available with this article online), this revealed that the *nhp6a/b* mutant strain was consistently more sensitive than the otherwise isogenic wild-type strain to UV light, the UV-mimetic drug 4-nitroquinoline N-oxide (4-NQO), H_2O_2, and—to a lesser extent—the DNA methylating agent methyl methane-sulphonate (MMS). Complementing the *nhp6a/b* double mutant strain with a plasmid carrying *NHP6A* largely suppressed the sensitivity of the *nhp6a/b* double mutant strain (Figure 1).

To further investigate the effects of Nhp6A/B proteins on DNA damage tolerance, we focused on lesions generated by UV irradiation. One way in which Nhp6A/B proteins might influence tolerance to UV is by facilitating the repair of UV lesions; alternatively, or in addition, they might alter chromatin structure in a manner that influences the initial yield of UV adducts. To differentiate between these possibilities, we took advantage of a monoclonal antibody, TDM2, which specifically recognizes thymine dimer adducts that are induced by UV light [11]. Thus, we treated wild-type and *nhp6a/b* mutant strains with UV light, extracted genomic DNA, spotted dilutions of this onto membranes, and then used the TDM2 antibody in dot-immunoblot assays to ascertain the extent and rate of repair of thymine dimer lesions. Notably, these analyses showed that both the wild-type and *nhp6a/b* mutant cells had completely removed all detectable thymine dimers before the 6 hr time point (Figures 2A and 2B). Moreover, assessment of the kinetics of TDM2 signal disappearance over time did not reveal any reproducible differences in the rates of repair between wild-type and *nhp6a/b* mutant strains (Figure 2B and data not shown). By contrast, *rad14* mutant cells—which are deficient in nucleotide excision repair—exhibited dramatically reduced rates of thymine dimer removal, with most of the damage still remaining even at late time points (Figure 2C). In parallel studies, we found that *nhp6a/b* mutant cells were proficient DNA damage checkpoint signaling in response to 25 μM 4-NQO, as Rad53 phosphorylation and Rad9 hyperphosphorylation were not impaired in the *nhp6a/b* mutant strain under these conditions. In addition, epistasis analysis indicated that Nhp6A/B do not affect the two major pathways of DNA DSB repair that are governed by Yku70 and Rad52 (data not shown). Consistent with these data, transcription of known DNA repair and DNA damage checkpoint genes does not appear to be significantly perturbed in the absence of Nhp6A/B [7].

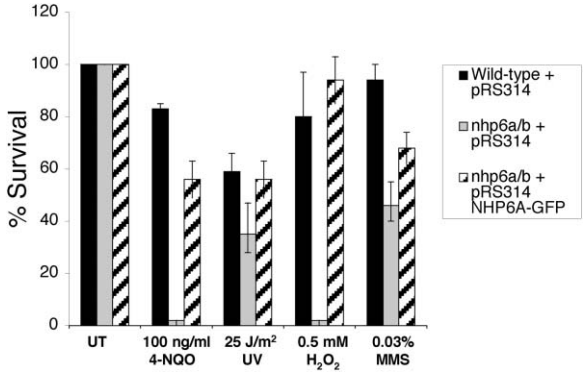

Figure 1. Hypersensitivity of the *nhp6a/b* Mutant Strain to DNA-Damaging Drugs

Survival of wild-type and *nhp6a/b* mutant strains in the presence of the indicated amount of drugs: disruption of *NHP6A/B* causes hypersensitivity to high doses of 4-NQO, UV, MMS, or H_2O_2. The number of colonies obtained is presented as percentage of those arising in the absence of drug. Complementation of *nhp6a/b* mutant strain with pRS314 NHP6A-GFP generally restores normal sensitivity to the different drugs tested.

During the above work, we noted that the amount of thymine dimers was consistently higher in samples derived from *nhp6a/b* mutant cultures than in those from control cultures, or from cultures of the *rad14* mutant strain (Figures 2A and 2D and data not shown). Further assays focusing on early time points after damage induction (Figure 2E and data not shown) revealed that such differences cannot be accounted for by disparities in initial repair rates; instead, they reflect differences in original thymine dimer yields. To confirm this and to rule out influences from potential differences in cell metabolism or cellular architecture on thymine dimer formation, we prepared spheroplasts from wild-type and *nhp6a/b* mutant strains, lysed these with detergent, treated the samples with UV, and then immediately extracted the DNA for analysis. As shown in Figure 2F, the samples prepared in this way from *nhp6a/b* mutant cells gave rise to higher levels of thymine dimers than those derived from the wild-type control. Taken together, these data imply that chromatin within *nhp6a/b* mutant cells is intrinsically more vulnerable to UV-induced thymine dimer formation than chromatin from wild-type strains and strongly suggest that this difference underlies the greater UV sensitivity of *nhp6a/b* mutant cells.

The increased susceptibility of DNA in *nhp6a/b* mutant strains toward UV light suggested that this might also be the case for endogenously arising DNA-damaging agents. If so, we reasoned that this might be manifested by higher levels of genomic instability. Consistent with this prediction, when we used an assay developed by Kolodner and colleagues to detect and quantify the formation of gross chromosomal rearrangements (GCRs) [12], we found that *nhp6a/b* mutant cells displayed a reproducible ~2-fold higher rate of GCR formation than the control strain (Table S1 in the Supplemental Data available with this article online), a result similar to that obtained by deletion of Ku or Sir proteins [13]. These results therefore indicate that Nhp6A/B proteins also protect the genome from spontaneous damage.

Previous work has established that increased geno-

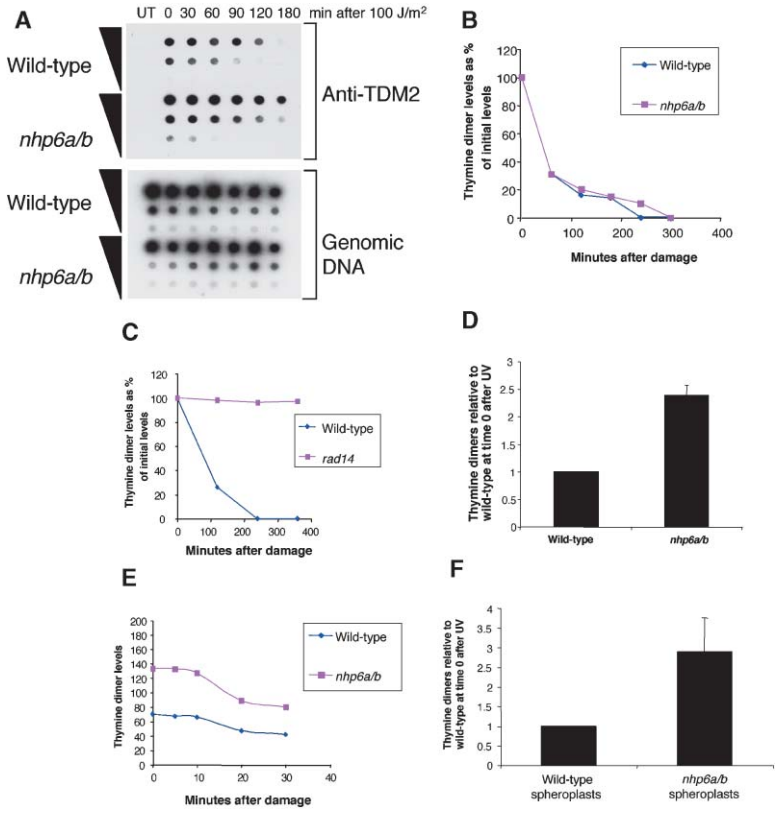

Figure 2. The *nhp6a/b* Mutant Strain Shows Higher Amounts of Thymine Dimers after UV Irradiation Than the Wild-Type Strain

(A) (Upper panel) The same amount of cells per strain was UV irradiated with 100 J/m² or not (UT). Samples were taken at the indicated time points, and DNA was extracted and spotted onto Hybond-N+ membrane for visualization of thymine dimers (anti-TDM2). (Bottom panel) The same membrane was hybridized with a probe specific for total genomic DNA extracted from the wild-type strain in order to quantify total DNA. (B, C, and E) Time course of thymine dimer repair. In (B) and (C), thymine dimer removal is measured as percentage relative to the initial amount of damage after UV. (D) Thymine dimer amount at time 0 after 100 J/m² in wild-type and *nhp6a/b* mutant strains, measured as described above. (F) Lysed spheroplasts from *nhp6a/b* mutant cells show higher levels of thymine dimers after UV irradiation.

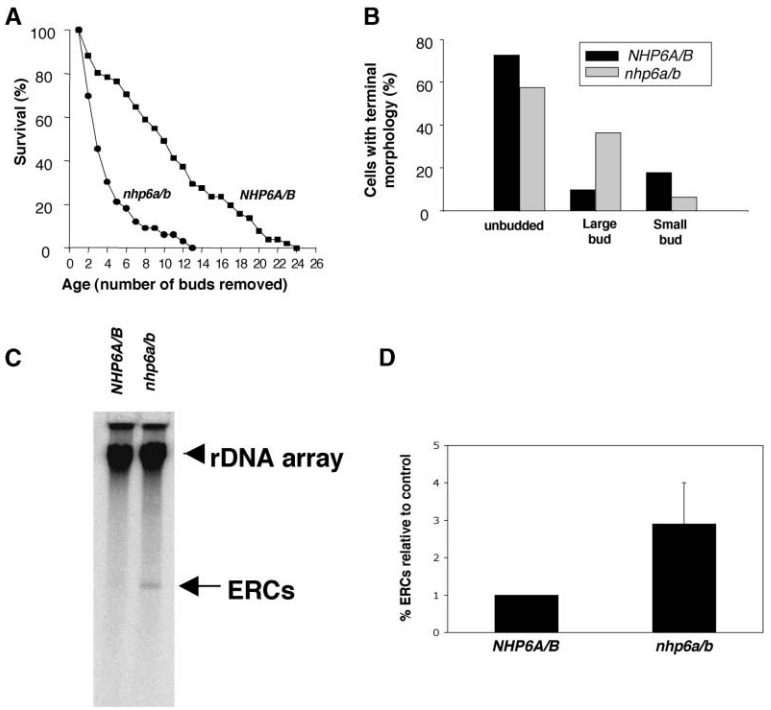

Figure 3. Nhp6A and Nhp6B Proteins Control Yeast Life Span

(A) Replicative age was defined as the number of buds removed from a mother yeast cell.

(B) Terminal morphology analysis of the cells used in the life span assays.

(C and D) Analysis of ERC accumulation in *nhp6a/b* mutant and control cells.

mic instability causing recombination between the rDNA repeat sequences can lead to decreased yeast cell life span [14]. We therefore tested the replicative potential of *nhp6a/b* mutant and control strains through monitoring—by microscopy and micromanipulation—the ability of mother cells to serially divide. This analysis revealed that the *nhp6a/b* mutant strain has a significantly ($p < 0.001$) shorter life span (mean of 3.3 and maximum of 12 buds removed; $n = 33$ cells) than the control strain (mean of 9.7 and maximum of 23 buds removed; $n = 51$ cells) and that only a minority of virgin *nhp6a/b* mutant cells ever produced a bud (Figure 3A). The 66% reduction in mean life span in *nhp6a/b* mutants is similar to that seen in the *sgs1*, *srs2*, and *sir2* hyperrecombination mutants, which have been reported to exhibit 57%, 55%, and 46% reductions, respectively [15–17]. Notably, terminal morphology analysis of the cells used in the life span studies revealed an increased incidence of cells senescing with a large bud attached, a phenotype that is seen in some strains exhibiting increased recombination, such as *sgs1* and *srs2* mutants [17, 18] (Figure 3B). Because reduced life span in *sir2* mutants (but not in *sgs1* mutants) is inversely correlated with the rate of generation of extrachromosomal rDNA circles (ERCs) that derive from recombination between the rDNA repeats, we analyzed ERC formation in the *nhp6a/b* mutant strain. As shown in Figures 3C and 3D, this revealed a reproducible increase in ERC formation in the *nhp6a/b* mutant strain as compared to the control strain. The magnitude of this increase was similar to that documented for *sir2* mutants, in which a doubling of ERC levels leads to shortened life span [15].

The presence of Nhp6A/B-related proteins in other organisms suggested to us that other members of this family, such as mammalian Hmgb1, might also possess genome-protective functions. To test this idea, we carried out cytogenetic analyses of primary mouse embryonic fibroblasts (MEFs) derived from *Hmgb1*$^{-/-}$ knockout embryos and, as controls, cells from their wild-type siblings. Strikingly, high levels of aneuploidy and spontaneous chromosome aberrations were observed in the *Hmgb1*$^{-/-}$ MEFs (Figure 4A and Table 1). Thus, in con-

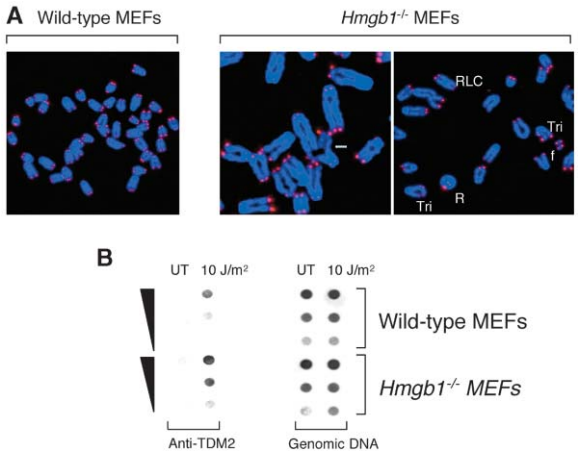

Figure 4. Chromosomal Abnormalities and Increased Rates of Aneuploidy Are Associated with Inactivation of Mouse *Hmgb1*

(A) For *Hmgb1*$^{-/-}$ MEFs, partial metaphase spreads are shown here; the metaphase spreads were stained with telomere probe to facilitate unambiguous identification of chromosome aberrations involved. RLC, Robertsonian fusion-like configuration; Tri, triradial-like structure; R, ring-like structure; f, fragments. The arrow points to a triradial-like structure.

(B) MEFs from *Hmgb1*$^{-/-}$ mice show higher levels of thymine dimers after UV irradiation than wild-type controls.

Table 1. Analysis of Rates of Chromosomal Aberrations in Wild-Type and *Hmgb1*$^{-/-}$ MEFs

Sample	Metaphases Analyzed	Aneuploid Cells	Total End-to-End Fusions[a]	Fragments[b]	Breaks[c]	Triradial-like Structures
Wild-type	25	0	0	0	0	0
Hmgb1$^{-/-}$	25	15 (60%)	5 (20%)	3 (12%)	3 (12%)	4 (12%)

Results from cytogenetic analysis of metaphase chromosomal spreads from primary MEFs are shown. Numbers in parentheses indicate the percent frequency.

[a] Includes one Robertsonian fusion-like configuration, one dicentric chromosome, and three ring-like structures.

[b] Includes centric and acentric fragments.

[c] Includes chromosome and chromatid breaks.

trast to wild-type MEFs—where no chromosomal aberrations were observed in the 25 metaphases analyzed—60% of *Hmgb1*$^{-/-}$ cells were aneuploid. *Hmgb1*$^{-/-}$ MEFs also exhibited chromosomal abnormalities, which included chromosome breaks, fragments, and end-to-end fusions; dicentrics; rings; and Robertsonian-like fusions (Figure 4A and Table 1). Furthermore, *Hmgb1*$^{-/-}$ MEFs displayed triradial-like structures, which are a consequence of reciprocal exchange of double-stranded DNA leading to chromatid exchange. These data therefore reveal that mouse Hmgb1 promotes genome stability and suggest that it might do this by acting in a similar manner to yeast Nhp6A/B proteins. In line with this idea, when we irradiated *Hmgb1*$^{+/+}$ and *Hmgb1*$^{-/-}$ cells with 10 J/m^2 of UV, extracted their DNA, spotted serial dilutions onto membranes, and analyzed them with the TDM2 antibody, we detected higher levels of initial damage in the cells lacking Hmgb1 than in the Hmgb1-proficient controls (Figure 4B).

Taken together, our results show that yeast Nhp6A/B proteins and mammalian Hmgb1 play important roles in promoting genome stability and suggest that they do this in analogous ways. Although the precise mechanism(s) by which Nhp6A/B and Hmgb1 help to reduce genome damage is not fully known, it seems likely that they do so through modulating local or higher-order chromatin structure. Indeed, HMGB family proteins are abundantly expressed in both yeast and mammalian cells, so they are present in sufficient quantities to perform such a global genome-protective function. Notably, however, we have been unable to identify reproducible differences between the chromatin structures of wild-type and *nhp6a/b* mutant strains in micrococcal nuclease digestion experiments (data not shown). In addition, previous work has reported that there are no differences in micrococcal nuclease accessibility between *Hmgb1*$^{-/-}$ MEFs and wild-type MEFs [19]. We therefore speculate that Nhp6A/B proteins and Hmgb1 do not protect genomic DNA by markedly influencing chromatin compaction but instead alter chromatin in a more subtle way in order to limit genome damage.

Experimental Procedures

Yeast Strains and Plasmids

The S288C strain bearing the *NHP6A* and *NHP6B* disruptions was provided by Michael Snyder [20]. *NHP6A* and *NHP6B* disruption in other strains was done by standard yeast protocols through PCR amplification of the cassettes from S288C (*nhp6a::URA3* and *nhp6b::HIS3*), transforming these into the relevant strain, and then confirming integration by PCR analysis of genomic DNA. When necessary, markers have been swapped. BY4741 and *rad14* BY4741 were from Euroscarf. For GCR and life span analysis, we used RDKY3733 containing a *SML1* disruption (provided by Richard Kolodner) [12]. pRS314 carrying NHP6A-GFP was a generous gift of Reid C. Johnson [21].

Drug Sensitivity and Chromosomal Rearrangement Assays

Drug sensitivity assays were performed on cultures that had been grown overnight in the appropriate medium at 30°C. Cultures were diluted to OD_{600} of 0.01 in water and plated by an automated spiral plater (DW Scientific) onto glucose medium with the appropriate drug. Colonies were counted after 4–5 days incubation at 30°C. Gross chromosomal rearrangement assays were done as described previously [12], and mutation rates were calculated as an average of three independent experiments using sets of five different cultures per strain.

Thymine Dimer Detection

Cells were grown overnight at 30°C and diluted to OD_{600} 1.5 the next morning. Medium was then washed away, and cells were resuspended in water to give equivalent cell concentrations for different cultures. After the suspensions were poured into Petri dishes, the cells were irradiated with UVC (100 J/m^2), resuspended in YPAD, and incubated again at 30°C. Samples (normally 10 ml) were taken at indicated time points, and DNA was extracted as follows: sample pellet was resuspended in 500 μl of lysis buffer (50 mM HEPES [pH 7.4], 1% Triton X-100, 0.1% sodium deoxycholate, 0.15 M NaCl), then cells were disrupted using a Fast Prep cell disrupter apparatus (Qbiogene) in the presence of glass beads. Supernatant was transferred to a new microcentrifuge tube and was then sonicated for 10 s at 25% output. Samples were centrifuged at 4°C for 15 min, and the resulting supernatant was incubated at 37°C in the presence of proteinase K (final concentration 0.1 μg/μl) for 10 min. DNA was finally phenol-chloroform extracted, ethanol precipitated, and resuspended in 100 μl of water. At this stage, the OD_{260} was taken, and three 5-fold dilutions starting from 5 μg of DNA were diluted to 50 μl in a final concentration of 0.2 M NaOH. Samples were then incubated at 37°C for 15 min, boiled, and spotted onto a Hybond N+ (Amersham Biosciences) membrane using a dot-blot apparatus. The membrane was dried at 80°C for 60 min, blocked with 1% milk (Marvel), and incubated overnight with an anti-thymine dimer (TDM2) antibody (provided by Tsukasa Matsunaga [11]). After unbound material was washed off, the primary antibody was detected using a horseradish peroxidase-conjugated rabbit anti-mouse IgG (Dako, Denmark) and visualized by chemiluminescence with the ECL reagent (Amersham Biosciences). Nonsaturated ECL chemiluminescence signals have been quantified using NIH image program.

Yeast Life Span Analysis

Strains were grown in YPD medium at 30°C to OD_{600} of 0.7–0.9, and then 2 μl of cultures were streaked on YPD plates and left at 30°C for several hours before being incubated at 4°C overnight. After this, cell doublets were moved to uninhabited regions of the plate. When these budded again, newly formed cells were removed by micromanipulation away and cataloged. The plates were incubated at 30°C during working hours and 4°C overnight. Life span was defined as number of daughter cells removed from the mother cell. Statistical significance of differences in life span was determined using the Mann-Whitney test.

For ERC accumulation analysis, DNA was isolated and electrophoresed at 20V for 24–30 hr in the absence of ethidium bromide. Transfers were probed with a ^{32}P-CTP-labeled 750 bp fragment of rDNA derived from a pGEMT-rDNA plasmid. ERCs were quantified by densitometry and corrected for loading differences by normalizing to total rDNA levels in the chromosomal array. The levels indicated are the averages from three independent experiments.

MEF Tissue Culture, Chromosome Analysis, and Thymine Dimer Measurements

Hmgb1$^{-/-}$ mice were described in [19]. MEFs were obtained from 14-day embryos deriving from crosses of completely syngenic (ten backcrosses with BALB/C mice) *Hmgb1* heterozygotes. *Hmgb1*$^{-/-}$ and $^{+/+}$ MEFs were derived from sibling embryos to minimize differences in embryo age or environmental conditions. MEFs were maintained in Dulbecco's modified Eagle's medium (DMEM) with 10% FBS, penicillin, streptomycin, and glutamine (all Gibco-BRL). Cells were grown at 37°C in an atmosphere containing 7% CO_2. Chromosome spreads were hybridized with a Cy-3-labeled $(CCCTAA)_3$ peptide nucleic acid (PNA) probe [22]. Metaphase spreads were captured using a Zeiss Axioplan 2 imaging fluorescence microscope, and the images were processed using ISIS karyotyping software (Metasystems, Germany). Gross chromosome rearrangements in 25 metaphases per sample were analyzed. All studies were carried out blind. For thymine dimer detection, on the day of the experiment medium was washed away, and cells were left in 1× PBS. Plates were irradiated with 10 J/m^2 or mock treated. After trypsinization, DNA was extracted with DNeasy Tissue kit (Qiagen) and quantified; then, three 5-fold dilutions starting from 1 μg of DNA were spotted onto Hybond-N+ membrane, and the assay was performed as described above except that the primary antibody was incubated at room temperature for 2 hr.

Supplemental Data

Supplemental Data including an additional figure and an additional table are available at http://www.current-biology.com/cgi/content/full/15/1/68/DC1/.

Acknowledgments

We thank Richard Kolodner for providing strains for GCR assays; Michael Snyder for the original *nhp6a/b* mutant strain; Reid C. Johnson for pRS314-NHP6A-GFP; and Tsukasa Matsunaga for TDM2 antibody. We also thank Lorenza Ronfani and CFCM staff (Milano) for mouse backcrossing and MEF derivation and Julia Coates, Jessica Downs, Serge Gravel, Veronique Smits, and Helena Santos-Rosa for helpful discussions. Research in the S.P.J. laboratory is funded by grants from Cancer Research UK, and S.G. is funded by a Cancer Research UK studentship. M.P.H. is supported by grants from Academic Research Fund; National University of Singapore; and Oncology Research Institute, NUMI, Singapore. M.E.B. is funded by the Associazione Italiana Ricerca sul Cancro (AIRC) and Ministero dell'Istruzione, Università e Ricerca. E.K. is supported by a BBSRC grant to A.M. F.d'A.d.F. is supported by AIRC.

Received: August 11, 2004
Revised: October 24, 2004
Accepted: October 25, 2004
Published: January 11, 2005

References

1. Kolodrubetz, D., Haggren, W., and Burgum, A. (1988). Amino-terminal sequence of a Saccharomyces cerevisiae nuclear protein, NHP6, shows significant identity to bovine HMG1. FEBS Lett. *238*, 175–179.
2. Allain, F.H., Yen, Y.M., Masse, J.E., Schultze, P., Dieckmann, T., Johnson, R.C., and Feigon, J. (1999). Solution structure of the HMG protein NHP6A and its interaction with DNA reveals the structural determinants for non-sequence-specific binding. EMBO J. *18*, 2563–2579.
3. Masse, J.E., Wong, B., Yen, Y.M., Allain, F.H., Johnson, R.C., and Feigon, J. (2002). The S. cerevisiae architectural HMGB protein NHP6A complexed with DNA: DNA and protein conformational changes upon binding. J. Mol. Biol. *323*, 263–284.
4. Formosa, T. (2003). Changing the DNA landscape: Putting a SPN on chromatin. Curr. Top. Microbiol. Immunol. *274*, 171–201.
5. Formosa, T., Eriksson, P., Wittmeyer, J., Ginn, J., Yu, Y., and Stillman, D.J. (2001). Spt16-Pob3 and the HMG protein Nhp6 combine to form the nucleosome-binding factor SPN. EMBO J. *20*, 3506–3517.
6. Yu, Y., Eriksson, P., and Stillman, D.J. (2000). Architectural transcription factors and the SAGA complex function in parallel pathways to activate transcription. Mol. Cell. Biol. *20*, 2350–2357.
7. Moreira, J.M., and Holmberg, S. (2000). Chromatin-mediated transcriptional regulation by the yeast architectural factors NHP6A and NHP6B. EMBO J. *19*, 6804–6813.
8. Bustin, M. (1999). Regulation of DNA-dependent activities by the functional motifs of the high-mobility-group chromosomal proteins. Mol. Cell. Biol. *19*, 5237–5246.
9. Agresti, A., and Bianchi, M.E. (2003). HMGB proteins and gene expression. Curr. Opin. Genet. Dev. *13*, 170–178.
10. Aidinis, V., Bonaldi, T., Beltrame, M., Santagata, S., Bianchi, M.E., and Spanopoulou, E. (1999). The RAG1 homeodomain recruits HMG1 and HMG2 to facilitate recombination signal sequence binding and to enhance the intrinsic DNA-bending activity of RAG1-RAG2. Mol. Cell. Biol. *19*, 6532–6542.
11. Mori, T., Nakane, M., Hattori, T., Matsunaga, T., Ihara, M., and Nikaido, O. (1991). Simultaneous establishment of monoclonal antibodies specific for either cyclobutane pyrimidine dimer or (6-4)photoproduct from the same mouse immunized with ultraviolet-irradiated DNA. Photochem. Photobiol. *54*, 225–232.
12. Myung, K., Datta, A., and Kolodner, R.D. (2001). Suppression of spontaneous chromosomal rearrangements by S phase checkpoint functions in *Saccharomyces cerevisiae*. Cell *104*, 397–408.
13. Chen, C., and Kolodner, R.D. (1999). Gross chromosomal rearrangements in Saccharomyces cerevisiae replication and recombination defective mutants. Nat. Genet. *23*, 81–85.
14. Sinclair, D.A., and Guarente, L. (1997). Extrachromosomal rDNA circles—a cause of aging in yeast. Cell *91*, 1033–1042.
15. Kaeberlein, M., McVey, M., and Guarente, L. (1999). The SIR2/3/4 complex and SIR2 alone promote longevity in Saccharomyces cerevisiae by two different mechanisms. Genes Dev. *13*, 2570–2580.
16. Mankouri, H.W., and Morgan, A. (2001). The DNA helicase activity of yeast Sgs1p is essential for normal lifespan but not for resistance to topoisomerase inhibitors. Mech. Ageing Dev. *122*, 1107–1120.
17. Mankouri, H.W., Craig, T.J., and Morgan, A. (2002). SGS1 is a multicopy suppressor of srs2: functional overlap between DNA helicases. Nucleic Acids Res. *30*, 1103–1113.
18. McVey, M., Kaeberlein, M., Tissenbaum, H.A., and Guarente, L. (2001). The short life span of Saccharomyces cerevisiae sgs1 and srs2 mutants is a composite of normal aging processes and mitotic arrest due to defective recombination. Genetics *157*, 1531–1542.
19. Calogero, S., Grassi, F., Aguzzi, A., Voigtlander, T., Ferrier, P., Ferrari, S., and Bianchi, M.E. (1999). The lack of chromosomal protein Hmg1 does not disrupt cell growth but causes lethal hypoglycaemia in newborn mice. Nat. Genet. *22*, 276–280.
20. Costigan, C., Kolodrubetz, D., and Snyder, M. (1994). NHP6A and NHP6B, which encode HMG1-like proteins, are candidates for downstream components of the yeast SLT2 mitogen-activated protein kinase pathway. Mol. Cell. Biol. *14*, 2391–2403.
21. Yen, Y.M., Roberts, P.M., and Johnson, R.C. (2001). Nuclear localization of the Saccharomyces cerevisiae HMG protein NHP6A occurs by a Ran-independent nonclassical pathway. Traffic *2*, 449–464.
22. Hande, M.P., Samper, E., Lansdorp, P., and Blasco, M.A. (1999). Telomere length dynamics and chromosomal instability in cells derived from telomerase null mice. J. Cell Biol. *144*, 589–601.